Bioactive films based on cuttlefish (Sepia officinalis) skin gelatin incorporated with cuttlefish protein hydrolysates: Physicochemical characterization and antioxidant properties

Hela Kchaou, Mourad Jridi, Nasreddine Benbettaïeb, Frédéric Debeaufort, Moncef Nasri

Bioactive films based on cuttlefish (*Sepia officinalis*) skin gelatin incorporated with cuttlefish protein hydrolysates: physicochemical characterization and antioxidant properties

Hela Kchaou[1], Mourad Jridi[1], Nasreddine Benbettaieb[2, 3], Frédéric Debeaufort[2, 3*], Moncef Nasri[1]

[1] National School of Engineering of Sfax, University of Sfax, Laboratory of Enzyme Engineering and Microbiology, P.O. Box 1173, Sfax 3038, Tunisia

[2]Univ. Bourgogne Franche-Comté AgroSup Dijon, UMR PAM A 02.102, 1 Esplanade Erasme, 21000 Dijon, France

[3]IUT-Dijon-Auxerre, BioEngineering Dpt., 7 blvd Docteur Petitjean, 20178 Dijon Cedex, France

***corresponding author :** Frédéric Debeaufort, Professor

e-mail : frederic.debeaufort@u-bourgogne.fr

Abstract

The objective of this study was to apply cuttlefish *(Sepia officinalis)* skin protein isolate (CSPI) and hydrolysates (CSPH), using commercial Savinase® and Purafect® enzymes, as bioactive additives in the elaboration of gelatin-based films. CSPH and CSPI enriched films were colored and exhibited a higher UV-barrier properties compared to gelatin film. In addition, compared to CSPI added film, an increase of the glass transition temperature by 20% and 4%, respectively, for Purafect and Savinase hydrolysates enriched films was noted. However, elongation at break decreased significantly for CSPH incorporated films by 2.5-fold. The tensile strength was reduced by 28.2% and 44.4% for Purafect and Savinase hydrolysates added films, respectively. Furthermore, a decrease of water contact angle by 45% and 51% for films added with Purafect and Savinase hydrolysates, respectively, was displayed compared to gelatin film. Interestingly, CSPH enriched films also displayed higher antioxidant potential than control gelatin films evaluated by several *in vitro* assays.

Keywords: Cuttlefish skin proteins and hydrolysates; Edible films; Functional properties; Antioxidant activity.

1. Introduction

In recent years, the interest in by-products (viscera, head, trimmings, bones and skin) from the fishing industry has been gradually increased, now being considered as a potential source of resources rather than a disposal waste (Alfaro, Balbinot, Weber, Tonial, & Machado-Lunkes, 2015). In order to valorize fish by-products, several bioactive molecules can be extracted from the skin of various marine species such as gelatin, protein isolate, etc. Indeed, fish proteins have advantageous filmogenic properties that can promote the development of films, such as the ability to form networks, plasticity, elasticity and good barrier to oxygen (Cortez-Vega, Pizato, de Souza, & Prentice, 2014).

Gelatin is an important biopolymer derived by hydrolysis from collagen, the primary protein component of animal connective tissues, including skin and tendon (Poppe, 1997). Gelatin is widely used by food, cosmetic and pharmaceutical industries because of its functional and technological properties. Fish gelatins have been also extensively studied as biodegradable biopolymers due to their good film forming ability leading to produce transparent, almost colorless, water-soluble and highly extensible films (Hosseini & Gómez-Guillén, 2018; Alfaro et al., 2015). Furthermore, these biodegradable films are considered as ecofriendly packaging reducing thereby plastic wastes (Hoque, Benjakul, & Prodpran, 2011a; Alinejad, Motamedzadegan, Rezaei, & Regenstein, 2017).

Gelatin films could be used as carrier agents for many types of additives such as antimicrobial agents in order to delay or prevent the growth of microorganisms on the products surface and thereby extend the shelf life and improve the safety of packaged foods (Etxabide, Uranga, Guerrero, & de la Caba, 2017). Antioxidants including plant extracts (Gómez-Guillén, Ihl, Bifani, Silva, & Montero, 2007; Hoque, Benjakul, & Prodpran, 2011b; Jridi et al., 2017), phenolic compounds (Bao, Xu, & Wang, 2009; Benbettaïeb et al., 2016), essential oils (Martucci, Gende, Neira, & Ruseckaite, 2015) or polysaccharides (Abdelhedi et

al., 2018) are additives often incorporated in fish gelatin films preparation to prevent or delay food oxidation. Recently, many studies dealt with the elaboration and characterization of protein hydrolysates from various marine sources. Protein hydrolysates, generally obtained by autolytic or heterolytic enzymatic hydrolysis process under controlled conditions from marine sources, are considered as bioactive peptides which are characterized by several biological activities including antioxidant (Abdelhedi et al., 2016; Nasri et al., 2013), antibacterial (Beaulieu, Bondu, Doiron, Rioux, & Turgeon, 2015), anti-diabetic (Harnedy et al., 2018), anti-hypertensive (Lassoued et al., 2015), anti-inflammatory (Ahn, Cho, & Je, 2015), cholesterol-lowering ability and immunomodulating effects (Nasri, 2017).

However, few studies were interested in protein hydrolysates incorporation as antioxidant agents into gelatin films. In this context, Giménez, Gómez-Estaca, Alemán, Gómez-Guillén, & Montero (2009) investigated the effect of the incorporation of giant squid gelatin hydrolysates on the antioxidant property of the gelatin film. Additionally, Alinejad et al. (2017) studied the influence of adding protein hydrolysates obtained from whitecheek shark on the physical-mechanical properties and antioxidant activity of bovine gelatin films. Abdelhedi et al. (2018) reported that bioactive blend and bilayer films based on gelatin and smooth-hound viscera proteins, incorporated or not with sulfated polysaccharide or smooth-hound peptides were successfully made and showed interesting antioxidant potential.

In a previous work, blend films based on cuttlefish (*Sepia officinalis*) skin gelatin (CSG) and protein isolate (CSPI) at different ratios were prepared and showed interesting antioxidant activity which is CSPI content dependent (Kchaou et al., 2017). In the present research, enzymatic hydrolysis was used in order to produce different protein hydrolysates (CSPH) from CSPI. Therefore, the aim of this study was to evaluate the effect of CSPH incorporation on the physical-chemical and antioxidant properties of gelatin films.

2. Materials and methods

2.1. Collection and preparation of cuttlefish skin

Cuttlefish (*S. officinalis*) by-products were obtained from the local fish market of Sfax City, Tunisia. Cuttlefish were collected from February to April at the golf of Gabes. The samples were packed in polyethylene bags, placed in ice and transported to the research laboratory within 30 min. Upon arrival, cuttlefish skins were washed several times with tap water to eliminate residues and dark ink and then stored at -20 °C in plastic bags until used for gelatin and protein isolate production.

2.2. Extraction of gelatin

Gelatin extraction was carried out from cuttlefish skin as described by Jridi et al. (2013a). Cuttlefish skin was first cut into small pieces (1 cm × 1 cm) and soaked in 0.05 M NaOH (1:10, w/v). The mixture was stirred for 2 h at room temperature (25±2 °C) and alkaline solution was changed every 30 min. The alkaline-treated skins were then washed with distilled water until a neutral pH was obtained. The prepared skins were soaked in 100 mM glycin–HCl buffer, (pH 2.0) with a solid/solvent ratio of 1:10 (w/v) for 18 h at room temperature (25±2 °C) (hydrolysis of collagen), and then treated at 50 °C for additional 18 h to extract the gelatin fractions. The supernatant of the obtained mixture was then freeze-dried (Moduloyd Freeze dryer, Thermo Fisher, USA) at -50 °C and 121 mbar during 72 h. The resulting cuttlefish skin gelatin (CSG) was used for film preparation.

2.3. Extraction of cuttlefish skin protein isolate

Protein isolate was extracted from cuttlefish skin as reported in our previous work (Kchaou et al., 2017) using the pH-shifting method. An aqueous dispersion of cuttlefish skin mince was first prepared, by solubilisation in distilled water. The pH was adjusted at 11.0

using 2 M NaOH solution for 30 min. The ratio cuttlefish mince and water was 1:3 (w/v). Solubilisation was maintained under continuous stirring at room temperature (25±2 °C). The resulting mixture was centrifuged. The obtained pellet containing the collagen underwent an acidic treatment with an HCl solution (1 M) at pH 2.0 for 15 minutes, followed by a thermal treatment at 50 °C for 1 hour to denature the triple helix collagen structure. The resulting mixture was centrifuged and the resulted supernatant was freeze-dried (at -50 °C and 121 mbar during 72 h) and referred to as cuttlefish skin protein isolate (CSPI).

2.4. Preparation of protein hydrolysates from CSPI

In order to obtain protein hydrolysates, CSPI was first dissolved in distilled water at 50 °C with a solid/solvent ratio of 1:4 (w/v). Then, the pH of the mixture was adjusted to the optimum value of each enzymatic activity (pH 10.0) by adding 4 N NaOH solution. Thereafter, protein isolate was subjected to enzymatic hydrolysis, using two exogenous enzymes, Savinase® and Purafect®, added at the same enzyme/protein ratio 6/1 (U/mg of protein) to compare their hydrolytic efficiencies. During the reaction (50 °C), the pH of the mixture was maintained constant (pH 10.0) by continuous addition of NaOH solution. After the achievement of the final digestion reaction time (7 h), the reactions were stopped by heating the different solutions at 95 °C for 20 min to inactivate the enzymes. The supernatants, corresponding to the different protein hydrolysates, were then collected, freeze-dried (at -50 °C and 121 mbar during 72 h) and stored at -20 °C for further use. Hydrolysates prepared using Savinase® and Purafect® were noted as Savinase and Purafect hydrolysates, respectively.

The degree of hydrolysis (DH), defined as the percent ratio of the number of peptide broken to the total number of bonds, was calculated based on the volume of NaOH added during the reaction, as described by Adler-Nissen (1986) using the following formula:

133 $$DH\ (\%) = \frac{(\mathrm{B\ x\ Nb}) * 100}{(\mathrm{MP\ x\ \alpha\ x\ h_{tot}})}$$

134 where B is the amount of NaOH consumed (mL), Nb is the normality of the base, MP is the
135 mass (g) of the protein (N = 6.25), α represents the average degree of dissociation of the α-
136 NH_2 groups in protein substrate ($\alpha = \frac{10^{\mathrm{pH-pK}}}{1+10^{\mathrm{pH-pK}}}$) and h_{tot} is the total number of peptide
137 bonds in the protein substrate and was assumed to be 8.6 meq/g (Alder-Nissen, 1986).

138 CSPI was hydrolyzed with Purafect® and Savinase® in order to elaborate bioactive
139 peptides. The hydrolysis kinetic curves (data not shown) displayed the same evolution,
140 characterized by a high rate of hydrolysis during the first hour, which was subsequently
141 slowing down with the reaction time and then reached a stationary phase. Regarding the
142 protease activity, Savinase® was more efficient than Purafect®. After 30 min of hydrolysis,
143 DHs values reached 6.92% and 3.84% for Savinase hydrolysate and Purafect hydrolysate,
144 respectively. After 7 h of hydrolysis, DHs values were 13.52% and 8.87% using Savinase®
145 and Purafect®, respectively. Indeed, the difference in DH values between Purafect and
146 Savinase hydrolysates is essentially due to the difference in the specificity of enzymes used.
147 During hydrolysis, Savinase® and Purafect® have different cleavage positions on polypeptide
148 chains. Savinase® and Purafect® produce therefore different hydrolysates (Bkhairia et al.,
149 2016). Typical hydrolysis curves were reported for protein hydrolysates of smooth hound
150 (*Mustelus mustelus*) (Abdelhedi et al., 2016), thornback ray (*Raja clavata*) (Lassoued et al.,
151 2015) and Goby (*Zosterissessor ophiocephalus*) (Nasri et al., 2013). In the following work,
152 we will focus only on hydrolysates obtained after 7 hours (end of hydrolysis).

153 *2.5. Films preparation*

154 CSG film forming solution was prepared by dissolving 4 g of CSG in 100 mL distilled
155 water. The mixture was heated at 60 °C for 30 min with continuous stirring and the pH was

156 adjusted to 5.5 with NaOH (0.5 M) to ensure fully dissolution and to obtain an homogeneous
157 colloidal solution of gelatin, that conduct to less crystalline and more homogeneous films.
158 CSG-enriched films were prepared by incorporating CSPH and CSPI at a concentration of
159 10% (w/w gelatin) in the film forming solutions. Then, the mixtures were gently stirred at
160 room temperature (25±2 °C) for 30 min. Glycerol was used as plasticizer at a concentration of
161 15% (w/w of gelatin). Films were obtained by casting each solution (25 mL) into plastic Petri
162 dishes (12 cm of side). Control films were made from the CSG film forming solutions without
163 adding CSPH and CSPI. Drying was then performed in a ventilated climatic chamber (KBF
164 240 Binder, ODIL, France) at 25 °C and 50% relative humidity (RH) for 24 h. Dried films
165 were manually peeled off from the surface and equilibrated at 25 °C and relative humidity
166 (RH) of 50% before analyses.

167 *2.6. Physical characterization of the films*

168 *2.6.1. Thickness*

169 Films thickness was measured using a digital thickness gauge (PosiTector 6000,
170 DeFelsko Corporation, USA). Five measurements at different locations were taken from each
171 film sample peeled from Petri dish, one from the center and four from the perimeter. The
172 average value was used in the calculation and taken into account for mechanical properties.

173 *2.6.2. Color*

174 Color of films was determined using a CIE colorimeter (CR-200; Minolta, Japan). A
175 white standard color plate (L_0^* = 97.5, a_0^* = -0.1, and b_0^* = 2.3) was used as background for
176 the color measurements of the films. Color of the films was expressed as L*
177 (lightness/brightness), a* (redness/greenness) and b* (yellowness/blueness) values. The

difference in color (ΔE*) for enriched films was calculated referred to the control CSG films according to the following equation:

$$\Delta E^* = \sqrt{(\Delta L^*)^2 + (\Delta a^*)^2 + (\Delta b^*)^2}$$

Where ΔL^*, Δa^* and Δb^* are the differences between the color parameters of the enriched films and those of control CSG films.

2.6.3. Light transmission

Film portions (1 cm x 3 cm) were placed in the test cell of a UV–Visible spectrophotometer (SAFAS UVmc). An empty test cell was used as a reference. UV-vis absorption spectra were recorded in the wavelength ranging from 200 to 800 nm. Results of UV-vis absorption spectra were then converted in terms of transmission spectra using the following formula:

$$T(\%) = 10^{(-A)}\text{x}100$$

Where T is the light transmission (%) and A representing the absorbance

2.6.4. FTIR spectroscopy

FTIR spectra of films were obtained using a Perkin-Elmer spectrometer (Spectrum 65, France) equipped with an attenuated total reflectance (ATR) accessory with a ZnSe crystal. 32 scans were collected with 4 cm^{-1} resolution in the wavenumber range 650-4000 cm^{-1}. Calibration was done using background spectrum recorded from the clean and empty cell at 25 °C. The Spectrum Suite ES software was used for FTIR data treatment.

2.6.5. Differential scanning calorimetry (DSC)

198 Thermal properties of films were studied using a differential scanning calorimeter
199 (DSC Q20, TA Instruments). Films (5 mg) were placed into aluminum pans, sealed and
200 subjected to a double heating-cooling cycle from -50 °C to 150 °C at a rate of 10 °C/min. The
201 empty aluminum pan was used as a reference. Nitrogen was used as purge gas at a flow rate
202 of 25 mL/min. Glass transition temperature (Tg) for each sample was then determined from
203 the mid-point of the second heating cycle using TA Universal Analysis 2000 software
204 (version 4.5 A, TA instruments).

205 *2.6.6. Thermogravimetric analysis (TGA)*

206 Thermogravimetric analysis was carried out to determine the thermal stability of the
207 film samples. This technique permits the continuous weighing of the film as a function of the
208 temperature rise in a controlled atmosphere (nitrogen). Thermogravimetric measurements
209 were performed using a TGA instrument (SDT Q 600). The samples (approximately 10 mg)
210 were heated from 25 to 600 °C at a heating rate of 5 °C/min under nitrogen atmosphere. Data
211 analysis was performed using TA Universal Analysis 2000 software (version 4.5 A, TA
212 instruments).

213 *2.6.7. Observation of film microstructure*

214 The cross-section morphology of film samples was determined using scanning
215 electron microscopy (SEM) (Hitachi S4800), at an angle of 90° with the surface, using
216 different magnifications. Prior to imaging the film cross-section, film samples were
217 cryofractured by immersion in liquid nitrogen and fixed on the SEM support using double
218 side adhesive tape, and observed under an accelerating voltage of 2.0 kV and an absolute
219 pressure of 60 Pa, after sputter coating with a 5 nm thick gold.

220 *2.6.8. Mechanical properties*

Tensile strength (TS, MPa) and elongation at break (EAB, %) of film samples were determined using a texture analyzer (TA. HD plus model, Stable MicroSystems, UK) with a 300 N load cell, according to the standard method ISO 527-3 (similar to the ASTM D882 method). Rectangular film samples with dimensions (2.5 cm x 8 cm) were cut using a standardized precision cutter (Thwing-Albert JDC Precision Sample Cutter) in order to get tensile test piece with an accurate width and parallel sides throughout the entire length. Before testing, all the samples were equilibrated for two weeks at 25 °C and 50% RH. Equilibrated films samples were then installed vertically in the extension grips of the testing machine and stretched uniaxially with a cross-head speed of 50 mm/min until breaking according to the ISO standard. The maximum load and the final extension at break were determined from the corresponding stress-strain curves and used for the calculation of TS and EAB as follows:

$$TS\ (MPa) = \frac{\text{Maximum force}}{\text{t x w}}$$

$$EAB(\%) = 100 \text{ x } \frac{(l - l_0)}{l_0}$$

where, t is the thickness (mm), w the width (mm) of films, l_0 the initial length of the film and l is the length of the film when it breaks. Measurements were carried out at room temperature (25 ± 2 °C) and six samples for each film formulation were tested.

2.6.9. Surface properties

The surface tension of films (γ_{film}) and its polar (γ_{film}^{P}) and dispersive (γ_{film}^{D}) components were determined using the Owens & Wendt (1969) method, using water (γ_{Liq} = 72.8 mN/m ; γ_{Liq}^{D} = 21.8 mN/m ; γ_{Liq}^{P} = 51 mN/m), ethylene glycol (γ_{Liq} = 47.7 mN/m ; γ_{Liq}^{D} = 30.9 mN/m; γ_{Liq}^{P} = 16.8 mN/m) and diiodomethane (γ_{Liq} = 50.8 mN/m ; γ_{Liq}^{D} = 50.8 mN/m ; γ_{Liq}^{P} = 0 mN/m) according the following equations:

$$\gamma_{S=}\gamma_S^{\mathbf{D}} + \gamma_S^{\mathbf{P}}$$

$$\gamma_{Liq}(1+\cos\theta) = 2\left(\sqrt{\gamma_{film}^{D} \times \gamma_{Liq}^{D}} + \sqrt{\gamma_{film}^{P} \times \gamma_{Liq}^{P}}\right)$$

Where θ, γ_{Liq}, $\gamma_{Liq}^{\mathbf{D}}$ and $\gamma_{Liq}^{\mathbf{P}}$ are respectively the contact angle, the surface tension, the dispersive and the polar components of the surface tension of the tested liquid; $\gamma_{film}^{\mathbf{P}}$ and $\gamma_{film}^{\mathbf{D}}$ are the polar and dispersive components of the surface tension of the film surface tested. The contact angle is expressed in degree and all the surface tension parameters are expressed in $mN.m^{-1}$.

Three liquids (water, ethylene glycol and diiodomethane), with well-known polar $\gamma_{Liq}^{\mathbf{P}}$ and dispersive $\gamma_{Liq}^{\mathbf{D}}$ contributions, were used. The contact angle measurements were carried out using the sessile drop method on a goniometer (Drop Shape Analyzer 30 from KrussGmbH), equipped with an image analysis software (ADVANCE). First, a droplet of each liquid (~2 µL) was deposited on the film surface with a precision syringe. The method is based on image processing and curve fitting for contact angle measurement from a theoretical meridian drop profile, determining contact angle between the baseline of the water drop and the tangent at the drop boundary. Then, the contact angle was measured at 0 time (<2 s) and at 30 s on both sides of the drop and averaged. Five measurements per film were carried out. All the tests were conducted in an environmental chamber with a constant environment at a temperature of 25±2 °C and a relative humidity of 50±1%.

2.7. In vitro antioxidant activity

2.7.1. Reducing power assay

The ability of CSPI, CSPH and films to reduce iron (III) was determined according to the method of Yıldırım, Mavi, & Kara (2001). The hydrolysates and the protein isolate were tested alone or in films with a concentration of 4.4 mg/mL. For this, a volume of 0.5 mL of each sample or small pieces of each film (10 mg), was mixed with 1.25 mL of 0.2 M phosphate buffer (pH 6.6) and 1.25 mL of 1% (w/v) potassium ferricyanide. The mixtures were then incubated for 30 min (3 h for the films) at 50 °C. After incubation, 1.25 mL of 10% (w/v) trichloroacetic acid was added to the mixtures which were centrifuged for 10 min at 10,000g. Finally, 1.25 mL of the supernatant solution of each sample mixture was mixed with 1.25 mL of distilled water and 0.25 mL of 0.1% (w/v) ferric chloride. After 10 min reaction time, the absorbance of the resulting solutions was measured at 700 nm using polystyrene spectrophotometry cuvettes. Higher absorbance of the reaction mixture indicated higher reducing power. The values are presented as the means of triplicate analyses.

2.7.2. DPPH free radical-scavenging activity

The DPPH free radical-scavenging activity of CSPH, CSPI and films was determined as described by Bersuder, Hole, & Smith (1998) with some modifications. 500µL of each sample or small pieces of each film (10 mg) were added to 375 µL of ethanol solution and 125 µL of 0.02 mM DPPH in ethanol. The mixtures were then incubated for 1 h at room temperature in the dark. Control tubes were assessed in the same manner without film samples. The reduction of DPPH radical was measured at 517 nm, using a UV–visible spectrophotometer.

The free radical-scavenging activity was calculated as follows:

$$DPPHscavenging(\%) = \frac{A_C - (A_S - A_b)}{A_C} x\ 100$$

where A_C is the absorbance of DPPH solution without addition of the films, A_S is the absorbance of DPPH solution containing the film samples and A_b is the absorbance of blank tubes containing film samples without addition of the DPPH solution.

A lower absorbance of the reaction mixture indicated a higher radical-scavenging activity. The test was carried out in triplicate.

2.7.3. β-carotene-linoleate bleaching assay

The ability of CSPH, CSPI and films to prevent β-carotene bleaching was determined according to the method of Koleva, van Beek, Linssen, de Groot, & Evstatieva (2002). 0.5 mg β-carotene in 1 mL chloroform was mixed with 25 µL of linoleic acid and 200 µL of Tween-40. The chloroform was completely evaporated under vacuum in a rotator evaporator at 40 °C, then 100 mL of double distilled water were added and the resulting mixture was vigorously stirred. The emulsion obtained was freshly prepared before each experiment. Aliquots (2.5 mL) of the β-carotene-linoleic acid emulsion were transferred into test tubes containing 0.5 mL from each sample or small pieces of each film (10 mg). The tubes were immediately placed in a water bath and incubated at 50 °C for 2 h. Thereafter, the absorbance of each sample was measured at 470 nm using polystyrene spectrophotometry cuvettes. The control tube was prepared in the same conditions by adding 0.5 mL of distilled water instead of the sample solution. The antioxidant activity was evaluated in terms of β-carotene bleaching inhibition using the following formula:

$$\beta - carotene\ bleaching\ inhibition\ (\%) = \left(1 - \left(\frac{A^0_{sample} - A^{120}_{sample}}{A^0_{control} - A^{120}_{control}}\right)\right) x100$$

where A^0: absorbance at t=0 min, A^{120}: absorbance at t=120 min. The test was carried out in triplicate.

309 *2.8. Statistical analysis*

310 Statistical analyses were performed with SPSS ver. 17.0, professional edition using ANOVA
311 analysis at a p level<0.05. Duncan's multiple range test (p-value<0.05) was used to detect
312 differences among mean values of all the parameters analyzed for the different films. A
313 standard deviation at the 90% confidence level was used to compare the DSC data for the
314 different films.

315 **3. Results and discussion**

316 *3.1. Functional properties of films*

317 *3.1.1. Color of films*

318 The color data of CSG films and those enriched by CSPI and CSPH are given in
319 Table 1. The highest L* and lowest b* values were detected with control films. Decreases in
320 L*-values and increases in a* and b*-values were observed in films, when CSPI and CSPH
321 were incorporated, indicating a decrease in lightness and an increase in browning color.
322 Enriched films are slightly brown compared to control films. The color difference was
323 confirmed by the calculation of ΔE* taking the gelatin film as reference. The obtained ΔE*-
324 values ranged from 5.47 to 6.94. Indeed, at the final moment of the enzymatic hydrolysis,
325 more colored peptides are generated. According to Dong et al. (2008), the longer hydrolysis
326 time probably accelerated the pigments oxidation and Maillard reaction. This may explain the
327 darkening and browning color of CSPH. Similarly, Nuanmano, Prodpran, & Benjakul (2015)
328 reported that the addition of fish gelatin hydrolysates with higher DH (95%) to fish
329 myofibrillar protein films leads to the same behaviour. Indeed, the yellowness may be due to
330 the amino groups ($-NH_2$) of the hydrolysate, which may interact with the carbonyl groups
331 (C=O) of lipid oxidation products in the polymeric matrix via the Maillard reaction,

particularly during drying of the film (Nuanmano et al., 2015; Rocha et al., 2018). Hasanzati Rostami, Motamedzadegan, Hosseini, Rezaei, & Kamali (2017) indicated a rise of the yellowish (b-values) and ΔE* values in gelatin films with the silver carp protein hydrolysate content. Furthermore, Lin et al. (2018) attributed the increase of yellowness to the higher content of lysine and histidine amino acids incorporated in the gelatin film matrix. Regarding the increase in redness with the addition of CSPH to gelatin films, this fact could be due to the initial colored compounds existing in CSPI (undigested protein) as it has been reported in previous work (Kchaou et al., 2017). Indeed, as a function of hydrolysis time, more peptides were generated, which may explain the darker color of CSPH.

3.1.2. UV and light barrier efficacy

Transmission of UV and visible light of gelatin films and those enriched with CSPI and CSPH was determined at selected wavelengths from 200 to 800 nm. Fig. 1 illustrated that prepared films have a high UV-barrier property in the range of (200-280 nm). This is attributed to the presence of some aromatic amino acids such as phenylalanine and tyrosine in the gelatin that absorb UV light (Jongjareonrak, Benjakul, Visessanguan, Prodpran, &Tanaka, 2006). Hoque et al. (2011a) reported similarly a very low transmission (0.01%) at 200 nm for cuttlefish (*Sepia pharaonis*) gelatin films. At 350 nm, light transmission decreases remarkably by about 56% for both hydrolysates incorporated films, respectively. These finding scould be explained by the fact that CSPH could contain more aromatic amino acids than the gelatin. In the visible range, control CSG film was the most transparent (≈ 80% transmission). The light transmission decreased with the incorporation of CSPI and CSPH in the UV (200-400 nm) and the visible (400-800 nm) ranges. Enriched films provided slighter barrier against light incidence and could be used as barrier packaging to protect packaged foods against light oxidative deterioration.

356 *3.1.3. FTIR spectra*

357 The infrared spectroscopy was used in this study in order to assess and determine the
358 interactions established between gelatin and CSPH or CSPI in the film matrix. Fig. 2 showed
359 the infrared spectra of gelatin film and those enriched with CSPI and protein hydrolysates.
360 Prepared films displayed similar spectra in the range of 700-1800 cm^{-1}. The main
361 characteristic absorption bands in gelatin films are located at 1560-1680 cm^{-1} (representing
362 C=C and C=O stretching of primary and secondary amine N-H band of amide-I), 1540-1610
363 cm^{-1} (assigned to NH of amide-II) and 1230-1340 cm^{-1} (assigned to aromatic primary amine,
364 C-N and N-H stretch of amide-III or vibrations of CH_2 groups of glycine) (Hoque et al.,
365 2011a). Moreover, all spectra of gelatin films showed major bands at approximately 3300-
366 3500 $cm^{-1}$and 2920-2945 cm^{-1}, corresponding to amide A (NH-stretching coupled with
367 hydrogen bonding) and amide B (asymmetric stretching vibration of =C–H and $–NH_3^+$). In
368 addition, a band located at 1040-1080 cm^{-1} was found in all film samples, corresponding to
369 the glycerol (-OH group) added as a plasticizer (Bergo & Sobral, 2007). The spectra did not
370 show significant difference in the position of the amides I, II and III. In addition, all the
371 samples of gelatins, protein isolates and protein hydrolysates derived from the same raw
372 material (cuttlefish skin). Thus, the added protein hydrolysates did not generate or suppress
373 the overall interactions present initially in gelatin films. However, for the amide A region, a
374 shift to lower wavenumbers was detected with the enriched films compared to gelatin film.
375 Indeed, amide A shifted from 3320 cm^{-1} to 3314 cm^{-1}, 3313 cm^{-1} and 3317 cm^{-1} with the
376 addition of CSPI, Purafect and Savinase hydrolysates, respectively. Generally, the decrease in
377 vibrational wavenumber and broadening of the OH and NH vibration bands could be linked to
378 the water content changes and water-biopolymer interactions via hydrogen bonding, which
379 could affect the network organization (Arfat, Benjakul, Prodpran & Osako, 2014; Kchaou et

al., 2017). This strengthening of the matrix by hydrogen bond is often revealed by a higher thermal stability or Tg

3.1.4. Thermal properties by DSC and TGA analyses

The thermal properties of gelatin films and those enriched with CSPI and CSPH were examined by DSC and the glass transition temperature (Tg) was determined from the second cycle of heating. The glass transition is associated with the molecular segmental motion of disordered (amorphous phase) structure, which undergoes from a brittle glassy solid state to a rubbery state (Nilsuwan, Benjakul, & Prodpran, 2018). As shown in Table 1, Tg value of control gelatin film was 58.4 °C and increased gradually to 59.5 °C and 61.8 °C with the addition of CSPI and Savinase hydrolysate, respectively. Tg value of control gelatin film (58.4 °C) was higher than that reported by Nilsuwan et al. (2018) for tilapia skin gelatin based films (45.5 °C) and lower than that stated by Jridi, Abdelhedi, Zouari, Fakhfakh, & Nasri (2019a) for films based on grey triggerfish skin gelatin (71.3 °C). The difference on Tg values for gelatin-based films depends on gelatin sources, compositions of film and process used (Tongnuanchan, Benjakul, Prodpran, & Nilsuwan, 2015).

Interestingly, Purafect hydrolysate incorporated films showed the highest Tg values which reached 71.4 °C. The increase in Tg values with the incorporation of CSPH could be explained by the establishment of interactions between hydrogen bonds of CSG and CSPH in the film matrix as displayed from FTIR experiments. An increase of the Tg value was also reported by Lin et al. (2018) with the addition of amino acids (lysine, arginine and histidine). Therefore the thermal stability of gelatin films was improved. However, Hasanzati Rostami et al. (2017) stated a decrease of Tg values with the addition of silver carp protein hydrolysates to fish gelatin films. The authors suggest that this decrease of Tg might be due to the lower molecular weight of protein hydrolysates which can position between protein chains themselves. Protein hydrolysates can also interfere with the protein-protein interaction, which

405 led to increasing the free volume between the polymer chains and the mobility of molecules
406 *i.e.* a plasticizing mechanism (Giménez et al., 2009).

407 The thermal stability of films was assessed by TGA at temperatures ranging from 25
408 to 600 °C. The TGA is a technique in which the mass change of a substance is measured
409 when it is subjected to a controlled temperature program. The thermal degradation
410 temperature, the weight loss (Δw) and the residue of films are presented in Table 1. From the
411 TGA curves (supplementary data), two main stages of weight loss were observed. The first
412 step of transformation starts from the ambient temperature until around 175 °C. This weight
413 loss (Δ*w1*) step corresponds to the loss of free and bound water in the films (above 100 °C)
414 and varied from 11% to 14%. The second stage of transformation is related to the thermal
415 degradation or the decomposition of the gelatin chains. The degradation temperatures (T_{max})
416 were ranging from 296.0 °C to 310.7 °C. In this stage, the weight loss (Δ*w2*) of films is
417 greater and ranged from 64.9% for gelatin films to around 60% for enriched films. The
418 residual mass at 600 °C, rose from 19% to about 23 and 25% when the protein hydrolysates
419 and CSPI were incorporated in gelatin films. The increase in T_{max} and residual mass values
420 suggest that the addition of CSPI and protein hydrolysates limited the thermal degradation of
421 gelatin films. The interactions between CSPH or CSPI and CSG in the film matrix, as
422 previously demonstrated by FTIR and DSC results, mostly yielded the stronger film network,
423 leading to higher heat resistance of enriched films than that of the CSG films (Arfat et al.,
424 2014). Their interactions mainly determine the thermal stability of enriched gelatin films by
425 hydrogen bonds (de Morais Lima et al., 2017).

426 *3.1.5. Microstructure*

427 Scanning Electron Microscopy observations were conducted in order to better
428 understand the microscopic structure of enriched films. Fig. 3 illustrates the scanning electron

429 micrographs of the cross-section of control gelatin film and those containing CSPI and
430 Purafect hydrolysate. The cross-section micrographs allow not only the observation of film
431 internal microstructures but they also contribute to a better knowledge of the film-forming
432 behavior of polymers. The micrographs revealed homogenous and uniform structure of
433 control and CSPI enriched films, suggesting therefore that the polymer and the additives
434 interacted well with each other. This allowed to form a cohesive and continuous matrix (de
435 Morais Lima et al., 2017). However, the micrograph of Purafect hydrolysate added film
436 displayed a relatively heterogeneous structure.

437 *3.1.6. Mechanical properties*

438 Results of tensile strength (TS) and elongation at break (EAB) of gelatin films and
439 those enriched with CSPI and CSPH are shown in Table 1. Among the different films, control
440 gelatin film showed the highest TS (22.67 MPa) and EAB (32.83%) values, followed by CSPI
441 enriched film, 22.09 MPa and 26.26%, respectively. The CSPH incorporation leads to a
442 significant decrease in the mechanical properties of gelatin films. Indeed, TS decreased by
443 30.1% and 45.8% for films added with Purafect and Savinase hydrolysates, respectively. The
444 EAB were around three-fold lower for CSPH enriched films compared to control film. The
445 decrease in both TS and EAB for CSPH incorporated films revealed the fragility of these
446 films, which are mechanically weaker and less deformable compared to control film. The
447 small peptides could be easily inserted in the protein network and establish hydrogen
448 bondings with the gelatin chains, which is detrimental for the chain–chain interactions. These
449 tend to decrease the density of intermolecular interactions and to increase the free volume
450 between gelatin chains (Giménez et al., 2009).

451 Our findings were in accordance with those of Jridi et al. (2013b) who indicated that
452 both TS and EAB values of CSG films decreased with the increase of pepsin used for gelatin

453 extraction (or the extent of gelatin hydrolysis). Moreover, Hasanzati Rostami et al. (2017)
454 reported that the mechanical strength was significantly reduced for gelatin films with the
455 addition of fish protein hydrolysate obtained from silver carp. In addition, Giménez et al.
456 (2009) reported that increasing the content of gelatin hydrolysates in the squid skin gelatin
457 films leads to a decrease of the mechanical resistance (puncture force) coupled to an increase
458 of the distensibility (puncture deformation) revealing a plasticization process. Furthermore,
459 microstructure results displayed a heterogeneous structure for Purafect hydrolysate enriched
460 films. This result correlates with the decrease in tensile strength and elongation at break for
461 CSPH incorporated films.

462 *3.1.7. Surface properties*

463 Surface properties of gelatin film and those enriched with CSPI and CSPH were
464 determined firstly by measuring their water contact angles (WCA) at 0 and 30 s as shown in
465 Fig. 4A. CSPI enriched film showed the highest initial water contact angle (WCA=114°)
466 followed by the gelatin film (88°). The higher WCA of CSPI added films could be explained
467 by the fact that CSPI contains more hydrophobic amino acids (leucine, isoleucine, valine,
468 methionine, tyrosine and phenylalanine, which represents 191.6 residues per 1000 residues)
469 compared to CSG that contains 80.4 residues per 1000 residue of hydrophobic acids (Kchaou
470 et al., 2017). The incorporation of the CSPH leads to a significant decrease in WCA values
471 which were in the range of 56-63°. Such results could be the consequence of the hydrophilic
472 character of the CSPH, which has shorter protein chains that contain polar amino acids able to
473 be re-oriented at the surface of the films. This provides a higher hydrophilicity. In this
474 context, Hoque et al. (2011a) indicated that protein hydrolysis could expose more carboxylic
475 group and amino group to the surface, which might then form hydrogen bonds with the water
476 molecules and lead to the higher hydrophilicity of the resulting films. Moreover, several
477 studies have shown that fish protein hydrolysates have excellent water holding capacity

478 favored by the presence of polar groups such as COOH and NH_2 generated by the enzymatic
479 hydrolysis. These polar groups have a substantial effect on the water absorption and
480 hydrophilicity (Wasswa, Tang, Gu, & Yuan, 2007; Kristinsson & Rasco, 2000). A decrease of
481 WCA values has been similarly indicated by Hasanzati Rostami et al. (2017) for gelatin films
482 incorporated with silver carp protein hydrolysates because of its high hydrophilic character.
483 Abdelhedi et al. (2018) reported that the smaller WCA obtained for gelatin films added with
484 smooth-hound peptides revealed their sensitivity against moisture. After 30 s, a slight
485 decrease of WCA was revealed for control gelatin films and those containing CSPI and
486 Purafect hydrolysate due to exclusively evaporation of the solvent in the surrounding
487 atmosphere that was not saturated with the liquid vapor (25 °C, 50% RH). For Savinase
488 hydrolysate enriched films, a higher decrease of WCA measured at 30 s was noted which
489 explain the faster absorption of the water droplet into the film surface.

490 In order to better understand the effect of CSPH incorporation on the gelatin films
491 surface properties, the surface tension, besides its polar and dispersive components, were
492 determined using two other liquids (ethylene glycol and diiodomethane) and results are given
493 in Fig. 4B. The shape of droplets deposited at the films surface are shown in Fig. 4C. Relative
494 contact angles values between the film surface and the solvent remained approximately
495 constant during 30 s (data not shown). Results presented in Fig. 4B displayed that control
496 gelatin films showed the highest dispersive component (35.8 mN/m) and the lowest polar
497 component (2.17 mN/m). Similarly, CSPI enriched films presented similarly a low polar
498 component (2.35 mN/m) but lower dispersive component (20.67 mN/m) compared to gelatin
499 films. After CSPH incorporation, the surface tension of incorporated films showed
500 modification due to the concomitant increase of polar component (16.04-22.55 mN/m) and
501 the decrease of dispersive component (20.61-23.91 mN/m). Thus, the CSPH addition
502 increased the wettability of gelatin films.

503 *3.2. Antioxidant activity of films*

504 The antioxidant activity was generally determined by different techniques that
505 involved direct or indirect measurement of the rate/extent of formation/decay of free radicals
506 (Antolovich, Prenzler, Patsalides, McDonald, & Robards, 2002). Indeed, the different assays
507 used for measuring the antioxidant activity are based on the fact that oxidation is largely
508 inhibited by the capture of initiating or propagating free radicals in the autoxidation process.
509 Therefore, they focus on monitoring the capacity of additives for radical capture or inhibition
510 of radical formation rather than on monitoring the actual oxidation itself (Benbettaïeb,
511 Debeaufort, & Karbowiak, 2018).

512 Three assays were conducted in order to evaluate the effect of CSPH and CSPI
513 incorporation on the antioxidant potential of gelatin films and to define the different
514 mechanisms of action of these additives (Fig. 5): reducing power, free radical-scavenging
515 activity (DPPH) and β-carotene bleaching inhibition.

516 First, the ability of CSPI and CSPH enriched films to reduce ferric ion (Fe^{3+}) was
517 investigated and data displayed that incorporated films exhibited higher activity than control
518 gelatin film (OD_{700nm} = 0.30) (Fig. 5A). The slight increase of the reducing power regarding
519 the enriched films was found to be more significant for those incorporated with CSPH.
520 However, the reducing activity of CSPH and CSPI in their free form was more important than
521 enriched films. These results could be explained either by the delayed release of the active
522 molecules from the gelatin film matrix or by the interactions established between the gelatin
523 and the active molecules in the film, which limited their release. Similarly, Giménez et al.
524 (2009) reported that squid gelatin hydrolysates showed lower antioxidant capacity in the
525 gelatin films than in the free form at the same amount added into the filmogenic solution
526 probably due to interactions between the peptides and gelatin film matrix formed via
527 hydrogen bonding.

528 Moreover, the antioxidant activity of gelatin films was highlighted by the DPPH free
529 radical-scavenging assay (Fig. 5B). Control gelatin film showed the lowest antioxidant
530 activity (39.88%). Whereas, the addition of CSPH and CSPI interestingly increased the
531 antioxidant capacity of gelatin films. Savinase and Purafect hydrolysates enriched films
532 displayed the highest radical scavenging activity (75.01% and 68.66%, respectively),
533 followed by CSPI enriched films (61.48%). This difference in the antioxidant activity
534 between enriched films could be ascribed to differences in film pore size which could affect
535 the amount of released compounds. In addition, it has been reported that the release of active
536 compounds from polymeric matrices is influenced mainly by the properties of both the
537 polymer and the active compound (López-de-Dicastillo et al., 2011). Moreover, the nature of
538 films seems to have as well a significant effect on films bioactivity and the blend film was
539 found to accelerate the release of the bioactive molecules from the film matrix (Abdelhedi et
540 al., 2018). In the free form, CSPI displayed the highest radical scavenging activity followed
541 by Savinase and Purafect hydrolysates. Indeed, the difference in protein hydrolysates and
542 isolate activity may be related to the difference in their molecular weight and to their
543 solubility in ethanol solution. CSPH showed higher antioxidant activity in the film matrix
544 than that in the free form. Indeed, the formation of protein-protein interactions or hydrogen
545 bonding between the film network and the added peptides may affect the antioxidant activity
546 of CSPH enriched films (Giménez et al., 2009). As the DPPH-radical scavenging assay is
547 based on the electron donating and hydrogen-bond donor properties, both of the CSPH
548 molecules and the presence of hydrogen bonding in CSPH enriched films could explain the
549 higher antioxidant activity of CSPH added films compared to their respective free form
550 (Benbettaïeb, Debeaufort, & Karbowiak, 2018).

551 Furthermore, the β-carotene-linoleate bleaching assay, which is based on the
552 disappearance of β-carotene color under thermally-induced oxidation (50 °C), was used to

553 evaluate the lipid peroxidation inhibitory activity of gelatin films. As shown in Fig. 5C, all
554 gelatin films prevent β-carotene bleaching by donating hydrogen atoms to peroxyl radicals of
555 linoleic acid. Control gelatin films exhibited the lowest antioxidant activity (29.42%) which
556 increased significantly and reached 52.75%, 48.63% and 44.12% with the addition of CSPI,
557 Savinase and Purafect hydrolysates, respectively. A low β-carotene bleaching inhibition
558 activity (20.35%) was also reported by Jridi et al.(2019b) in the case of grey triggerfish skin
559 gelatin films. Regarding the free form, CSPI, Savinase and Purafect hydrolysates displayed
560 high β-carotene bleaching with percentages of inhibition of 96.79±0.55%, 95.03±0.34% and
561 90.08±1.14%, respectively. Thus, CSPH and CSPI contain probably hydrogen or electrons
562 donating peptides that are able to stabilize the free radicals. However, the higher antioxidant
563 activity of active molecules in the free form suggest that it will be better to use CSPH or CSPI
564 directly in foods rather than to incorporate them into packaging due to their delayed release.
565 Natural antioxidant activity was similarly reported for fish gelatin based films from
566 different species (sole, catfish or cuttlefish), which has been mainly attributed to the peptide
567 fraction of such protein, probably elaborated during the gelatin extraction process (Gómez-
568 Estaca, Giménez, Montero, & Gómez-Guillén, 2009; Jridi et al., 2017).

569 **4. Conclusion**

570 This study investigates the effect of CSPH incorporation in gelatin films properties.
571 The addition of CSPH led to colored films with lower homogenous microstructure, higher
572 UV-barrier property and Tg values, compared to CSPI enriched film. However, mechanical
573 properties and hydrophobicity decreased for CSPH added films compared to gelatin and CSPI
574 enriched films. Furthermore, the antioxidant activity of the resulting enriched films was
575 enhanced, suggesting their possible potential use as active packaging against packaged foods
576 oxidation.

Acknowledgments and funding sources

The co-tutelle PhD of Ms Kchaou is supported by the Utique PHC program (project SeaCoatPack) N° 39290YK of Campus France and N° 18G0903 of the CMCU funded by the Ministries of Education and Research of both France and Tunisia and the French Embassy in Tunisia. The authors wish to thank the colleagues from the PAM-PCAV laboratory for their precious collaboration and help, and also thank ESIREM (Engineering School of Materials of the University of Burgundy) for the facilitated access to equipment and devices. The authors wish also to thank the European Institute of Membranes, UMR CNRS 5635, University of Montpellier for the access to scanning electron microscopy. This work was also supported by the Regional Council of Bourgogne –Franche Comté and the "Fonds Européen de Développement Régional (FEDER)" who invested in lab equipment's.

References

Abdelhedi, O., Jridi, M., Jemil, I., Mora, L., Toldrá, F., Aristoy, M.-C., Boualga, A., Nasri, M., & Nasri, R. (2016). Combined biocatalytic conversion of smooth hound viscera: Protein hydrolysates elaboration and assessment of their antioxidant, anti-ACE and antibacterial activities. *Food Research International, 86*, 9-23.

Abdelhedi, O., Nasri, R., Jridi, M., Kchaou, H., Nasreddine, B., Karbowiak, T., Debeaufort, F., & Nasri, M. (2018). Composite bioactive films based on smooth-hound viscera proteins and gelatin: Physicochemical characterization and antioxidant properties. *Food Hydrocolloids, 74*, 176-186.

Adler-Nissen, J. (1986). A review of food hydrolysis specific areas. In: Adler-Nissen J (ed) Enzymic hydrolysis of food proteins, Elsevier Applied Science Publishers, Copenhagen, pp 57–109.

601 Ahn, C.-B., Cho, Y.-S., & Je, J.-Y. (2015). Purification and anti-inflammatory action of
602 tripeptide from salmon pectoral fin byproduct protein hydrolysate. *Food Chemistry,*
603 *168*, 151-156.
604 Alfaro, A. d. T., Balbinot, E., Weber, C. I., Tonial, I. B., & Machado-Lunkes, A. (2015). Fish
605 gelatin: characteristics, functional properties, applications and future potentials. *Food*
606 *Engineering Reviews, 7*, 33-44.
607 Alinejad, M., Motamedzadegan, A., Rezaei, M., & Regenstein, J. M. (2017). Gelatin films
608 containing hydrolysates from whitecheek shark (*Carcharhinus dussumieri*) meat.
609 *Journal of Aquatic Food Product Technology, 26,* 420-430.
610 Antolovich, M., Prenzler, P.D., Patsalides, E., McDonald, S., & Robards, K. (2002). Methods
611 for testing antioxidant activity. *Analyst, 127,* 183-198.
612 Arfat, Y. A., Benjakul, S., Prodpran, T., & Osako, K. (2014). Development and
613 characterization of blend films based on fish protein isolate and fish skin gelatin. *Food*
614 *Hydrocolloids, 39,* 58-67.
615 Bao, S., Xu, S., & Wang, Z. (2009). Antioxidant activity and properties of gelatin films
616 incorporated with tea polyphenol-loaded chitosan nanoparticles. *Journal of the*
617 *Science of Food and Agriculture, 89*, 2692-2700.
618 Beaulieu, L., Bondu, S., Doiron, K., Rioux, L.-E., & Turgeon, S. L. (2015). Characterization
619 of antibacterial activity from protein hydrolysates of the macroalga *Saccharina*
620 *longicruris* and identification of peptides implied in bioactivity. *Journal of Functional*
621 *Foods, 17*, 685-697.
622 Benbettaïeb, N., Chambin, O., Assifaoui, A., Al-Assaf, S., Karbowiak, T., & Debeaufort, F.
623 (2016). Release of coumarin incorporated into chitosan-gelatin irradiated films. *Food*
624 *Hydrocolloids*, *56*, 266-276.

625 Benbettaïeb, N., Debeaufort, F., & Karbowiak, T. (2018). Bioactive edible films for food
626 applications: Mechanisms of antimicrobial and antioxidant activity. *Critical Reviews*
627 *in Food Science and Nutrition*, 1–25.
628 Bergo, P., & Sobral, P. J. A. (2007). Effects of plasticizer on physical properties of pigskin
629 gelatin films. *Food Hydrocolloids, 21*, 1285-1289.
630 Bersuder, P., Hole, M., & Smith, G. (1998). Antioxidants from a heated histidine-glucose
631 model system. I: Investigation of the antioxidant role of histidine and isolation of
632 antioxidants by high-performance liquid chromatography. *Journal of the American Oil*
633 *Chemists' Society, 75*, 181-187.
634 Bkhairia, I., Ben Slama-Ben Salem, R., Nasri, R., Jridi, M., Ghorbel, S., & Nasri, M. (2016).
635 In vitro antioxidant and functional properties of protein hydrolysates from golden grey
636 mullet prepared by commercial, microbial and visceral proteases. *Journal of Food*
637 *Science and Technology*, *53,* 2902–2912.
638 Cortez-Vega, W.R., Pizato, S., de Souza, J.T.A., & Prentice, C. (2014). Using edible coatings
639 from Whitemouth croaker (*Micropogonias furnieri*) protein isolate and organo-clay
640 nanocomposite for improve the conservation properties of fresh-cut 'Formosa'papaya.
641 *Innovative Food Science and Emerging Technologies, 22,* 197–202.
642 da Rocha, M., Alemán, A., Romani, V. P., López-Caballero, M. E., Gómez-Guillén, M. C.,
643 Montero, P., & Prentice, C. (2018). Effects of agar films incorporated with fish protein
644 hydrolysate or clove essential oil on flounder (*Paralichthys orbignyanus*) fillets shelf-
645 life. *Food Hydrocolloids, 81*, 351-363.
646 de Morais Lima, M.; Bianchini, D.; Guerra Dias, A.; Da Rosa Zavareze, E.; Prentice, C.; Da
647 Silveira Moreira, A. (2017). Biodegradable films based on chitosan, xanthan gum,and
648 fish protein hydrolysate. *Journal of Applied Polymer Science, 134,* 1-9.

649 Dong, S., Zeng, M., Wang, D., Liu, Z., Zhao, Y., & Yang, H. (2008). Antioxidant and
650 biochemical properties of protein hydrolysates prepared from Silver carp
651 (*Hypophthalmichthys molitrix*). *Food Chemistry, 107,* 1485-1493.
652 Etxabide, A., Uranga, J., Guerrero, P., & de la Caba, K. (2017). Development of active gelatin
653 films by means of valorisation of food processing waste: A review. *Food*
654 *Hydrocolloids, 68*, 192-198.
655 Giménez, B., Gómez-Estaca, J., Alemán, A., Gómez-Guillén, M. C., & Montero, M. P.
656 (2009). Improvement of the antioxidant properties of squid skin gelatin films by the
657 addition of hydrolysates from squid gelatin. *Food Hydrocolloids, 23*, 1322-1327.
658 Gómez-Estaca, J., Giménez, B., Montero, P., & Gómez-Guillén, M. C. (2009). Incorporation
659 of antioxidant borage extract into edible films based on sole skin gelatin or a
660 commercial fish gelatin. *Journal of Food Engineering, 92,* 78-85.
661 Gómez-Guillén, M. C., Ihl, M., Bifani, V., Silva, A., & Montero, P. (2007). Edible films
662 made from tuna-fish gelatin with antioxidant extracts of two different murta ecotypes
663 leaves (*Ugni molinae* Turcz). *Food Hydrocolloids, 21*, 1133-1143.
664 Harnedy, P. A., Parthsarathy, V., McLaughlin, C. M., O'Keeffe, M. B., Allsopp, P. J.,
665 McSorley, E. M., O'Harte, F. P. M., & FitzGerald, R. J. (2018). Atlantic salmon
666 (*Salmo salar*) co-product-derived protein hydrolysates: A source of antidiabetic
667 peptides. *Food Research International*, *106*, 598-606.
668 Hasanzati Rostami, A., Motamedzadegan, A., Hosseini, S.E., Rezaei, M., & Kamali, A.
669 (2017). Evaluation of plasticizing and antioxidant properties of silver carp protein
670 hydrolysates in fish gelatin film. *Journal of Aquatic Food Product Technology, 26*,
671 457–467.

672 Hoque, M. S., Benjakul, S., & Prodpran, T. (2011a). Effects of partial hydrolysis and
673 plasticizer content on the properties of film from cuttlefish (*Sepia pharaonis*) skin
674 gelatin. *Food Hydrocolloids, 25*, 82-90.
675 Hoque, M. S., Benjakul, S., & Prodpran, T. (2011b). Properties of film from cuttlefish (*Sepia*
676 *pharaonis*) skin gelatin incorporated with cinnamon, clove and star anise extracts.
677 *Food Hydrocolloids, 25*, 1085-1097.
678 Hosseini, S. F., & Gómez-Guillén, M. C. (2018). A state-of-the-art review on the elaboration
679 of fish gelatin as bioactive packaging: Special emphasis on nanotechnology-based
680 approaches. *Trends in Food Science & Technology, 79,* 125-135.
681 Jongjareonrak, A., Benjakul, S., Visessanguan, W., Prodpran, T., & Tanaka, M. (2006).
682 Characterization of edible films from skin gelatin of brownstripe red snapper and
683 bigeye snapper. *Food Hydrocolloids, 20*, 492-501.
684 Jridi, M., Abdelhedi, O., Zouari, N., Fakhfakh, N., & Nasri, M. (2019a). Development and
685 characterization of grey triggerfish gelatin/agar bilayer and blend films containing
686 vine leaves bioactive compounds. *Food Hydrocolloids*, *89*, 370-378.

687 Jridi, M., Boughriba, S., Abdelhedi, O., Nciri, H., Nasri, R., Kchaou, H., Kaya, M., Sebai, H.,
688 Zouari, N., & Nasri, M. (2019b). Investigation of physicochemical and antioxidant
689 properties of gelatin edible film mixed with blood orange (*Citrus sinensis*) peel
690 extract. *Food Packaging and Shelf Life, 21,* 100342.

691 Jridi, M., Sellimi, S., Bellassoued, K., Beltaief, S., Souissi, N., Mora, L., Toldra, F., Elfeki,
692 A., Nasri, M., & Nasri, R. (2017). Wound healing activity of cuttlefish gelatin gels and
693 films enriched by henna (*Lawsonia inermis*) extract. *Colloids and Surfaces A:*
694 *Physicochemical and Engineering Aspects, 512*, 71-79.
695 Jridi, M., Nasri, R., Lassoued, I., Souissi, N., Mbarek, A., Barkia, A., & Nasri, M. (2013a).
696 Chemical and biophysical properties of gelatins extracted from alkali-pretreated skin

of cuttlefish (*Sepia officinalis*) using pepsin. *Food Research International, 54*, 1680-1687.

Jridi, M., Souissi, N., Mbarek, A., Chadeyron, G., Kammoun, M., & Nasri, M. (2013b). Comparative study of physico-mechanical and antioxidant properties of edible gelatin films from the skin of cuttlefish. *International Journal of Biological Macromolecules, 61*, 17-25.

Kchaou, H., Jridi, M., Abdelhedi, O., Nasreddine, B., Karbowiak, T., Nasri, M., & Debeaufort, F. (2017). Development and characterization of cuttlefish (*Sepia officinalis*) skin gelatin-protein isolate blend films. *International Journal of Biological Macromolecules, 105*, 1491-1500.

Khemakhem, I., Abdelhedi, O., Trigui, I., Ayadi, M. A., & Bouaziz, M. (2018). Structural, antioxidant and antibacterial activities of polysaccharides extracted from olive leaves. *International Journal of Biological Macromolecules, 106*, 425-432.

Koleva, I. I., van Beek, T. A., Linssen, J. P. H., de Groot, A., & Evstatieva, L. N. (2002). Screening of plant extracts for antioxidant activity: a comparative study on three testing methods. *Phytochemical Analysis*, *13*, 8-17.

Kristinsson, H. G., & Rasco, B. A. (2000). Fish protein hydrolysates: Production, biochemical and functional properties. *Critical Reviews in Food Science and Nutrition, 40*, 43–81.

Lassoued, I., Mora, L., Nasri, R., Jridi, M., Toldrá, F., Aristoy, M.-C., Barkia, A., & Nasri, M. (2015). Characterization and comparative assessment of antioxidant and ACE inhibitory activities of thornback ray gelatin hydrolysates. *Journal of Functional Foods, 13*, 225-238.

Lin, J., Wang, Y., Pan, D., Sun, Y., Ou, C., & Cao, J. (2018). Physico-mechanical properties of gelatin films modified with Lysine, Arginine and Histidine. *International Journal of Biological Macromolecules, 108*, 947-952.

López-de-Dicastillo, C., Nerín, C., Alfaro, A., Catalá, R., Gavara, R., & Hernández- Muñóz, P. (2011). Development of new antioxidant active packaging films based on ethylene vinyl alcohol copolymer (EVOH) and green tea extract. *Journal of Agricultural and Food Chemistry, 59*, 7832-7840.

Martucci, J. F., Gende, L. B., Neira, L. M., & Ruseckaite, R. A. (2015). Oregano and lavender essential oils as antioxidant and antimicrobial additives of biogenic gelatin films. *Industrial Crops and Products, 71*, 205-213.

Nasri, M. (2017). Chapter four - Protein hydrolysates and biopeptides: production, biological activities, and applications in foods and health benefits. A review. *Advances in Food and Nutrition Research*, *81,* 109-159.

Nasri, R., Younes, I., Jridi, M., Trigui, M., Bougatef, A., Nedjar-Arroume, N., Dhulster, P., Nasri, M., & Karra-Châabouni, M. (2013). ACE inhibitory and antioxidative activities of Goby (*Zosterissessor ophiocephalus*) fish protein hydrolysates: Effect on meat lipid oxidation. *Food Research International, 54*, 552-561.

Nilsuwan, K., Benjakul, S., & Prodpran, T. (2018). Properties and antioxidative activity of fish gelatin-based film incorporated with epigallocatechin gallate. *Food Hydrocolloids, 80*, 212-221.

Nuanmano, S., Prodpran, T., & Benjakul, S. (2015). Potential use of gelatin hydrolysate as plasticizer in fish myofibrillar protein film. *Food Hydrocolloids, 47*, 61-68.

Owens, D. K., & Wendt, R. C. (1969). Estimation of the surface free energy of polymers. *Journal of Applied Polymer Science, 13*, 1741-1747.

Tongnuanchan, P., Benjakul, S., Prodpran, T., & Nilsuwan, K. (2015). Emulsion film based on fish skin gelatin and palm oil: Physical, structural and thermal properties, *Food Hydrocolloids, 48*, 248-259.

746 Wasswa, J., Tang, J., Gu, X.-h., and Yuan, X.-q. (2007). Influence of the extent of enzymatic
747 hydrolysis on the functional properties of protein hydrolysate from grass carp
748 (*Ctenopharyngodon idella*) skin. *Food Chemistry, 104*, 1698-1704.
749 Wu, H.-C., Chen, H.-M., & Shiau, C.-Y. (2003). Free amino acids and peptides as related to
750 antioxidant properties in protein hydrolysates of mackerel (*Scomber austriasicus*).
751 *Food Research International, 36*, 949-957.
752 Yıldırım, A., Mavi, A., & Kara, A. A. (2001). Determination of antioxidant and antimicrobial
753 activities of Rumex crispus L. extracts. *Journal of Agricultural and Food Chemistry,*
754 *49*, 4083-4089.

755

756

757

Fig. 1

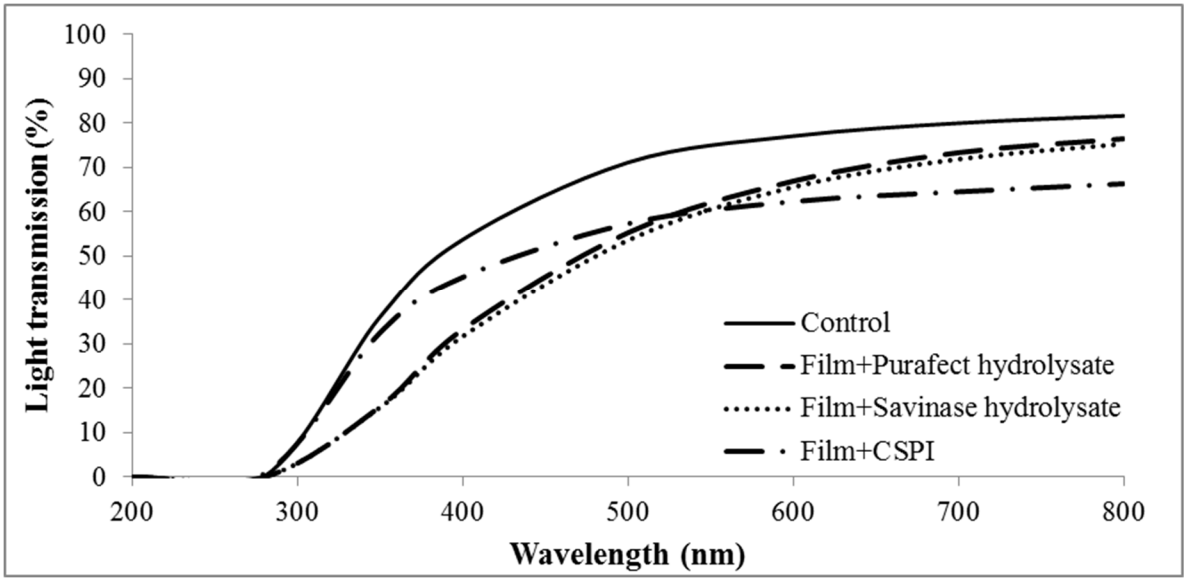
Light transmission (%)
100
90
80
70
60
50
40
30
20
10
0
200
300
400
500
600
700
800
Wavelength (nm)
Control
Film+Purafect hydrolysate
Film+Savinase hydrolysate
Film+CSPI

Fig. 2

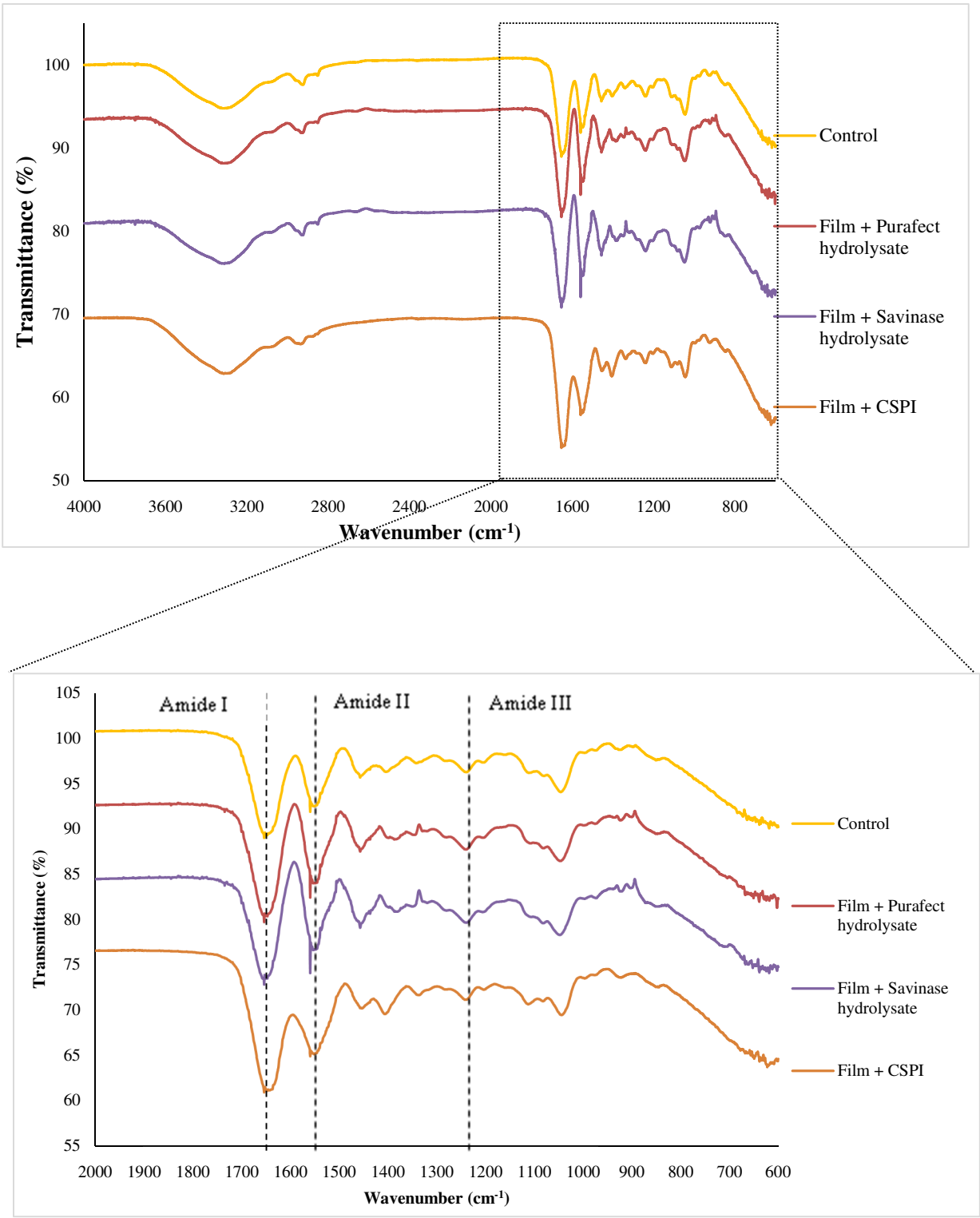
Transmittance (%)
100
90
80
70
60
50
4000
3600
3200
2800
2400
2000
1600
1200
800
Wavenumber (cm-1)
Control
Film + Purafect hydrolysate
Film + Savinase hydrolysate
Film + CSPI
Amide I
Amide II
Amide III
105
100
95
90
85
80
75
70
65
60
55
2000
1900
1800
1700
1600
1500
1400
1300
1200
1100
1000
900
800
700
600
Wavenumber (cm-1)
Control
Film + Purafect hydrolysate
Film + Savinase hydrolysate
Film + CSPI

Fig. 3

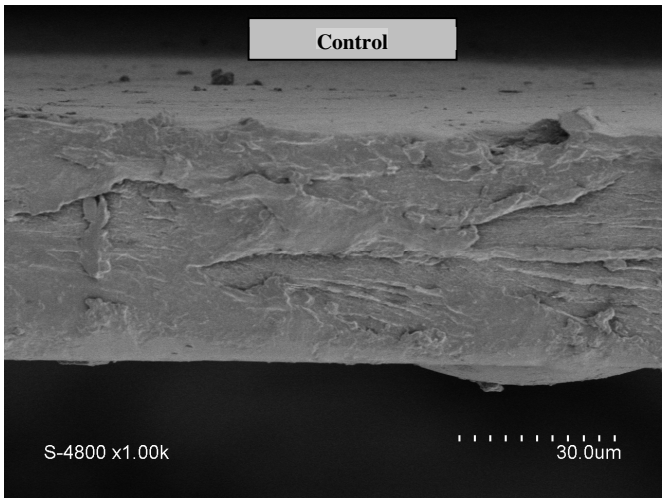
Control
S-4800 x1.00k
30.0um

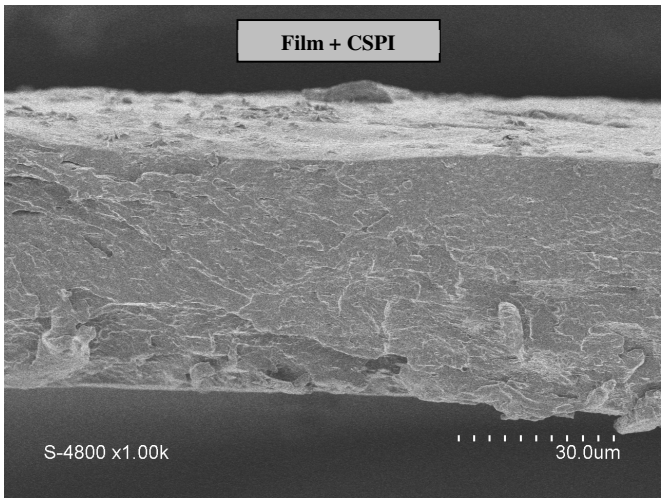
Film + CSPI
S-4800 x1.00k
30.0um

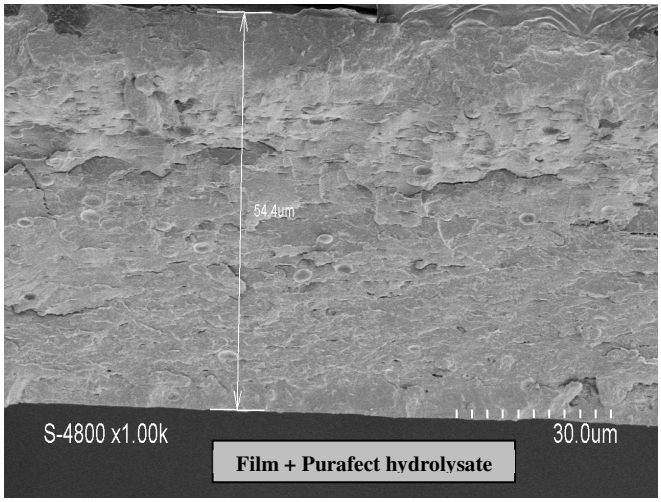
54.4um
S-4800 x1.00k
30.0um
Film + Purafect hydrolysate

Fig. 4

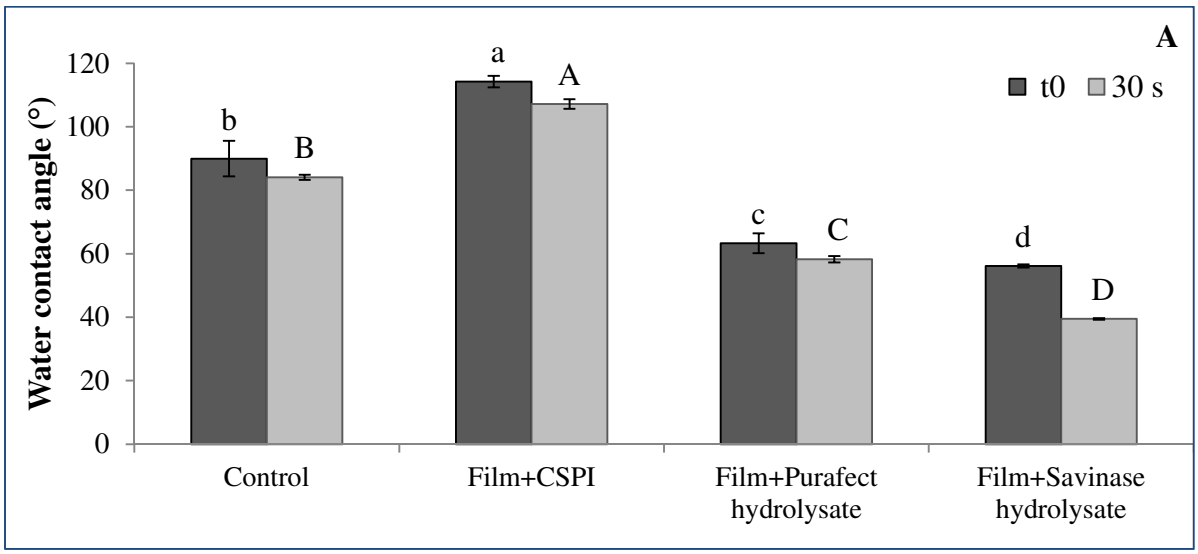
A
Water contact angle (°)
120
100
80
60
40
20
0
t0
30 s
a
A
b
B
c
C
d
D
Control
Film+CSPI
Film+Purafect hydrolysate
Film+Savinase hydrolysate

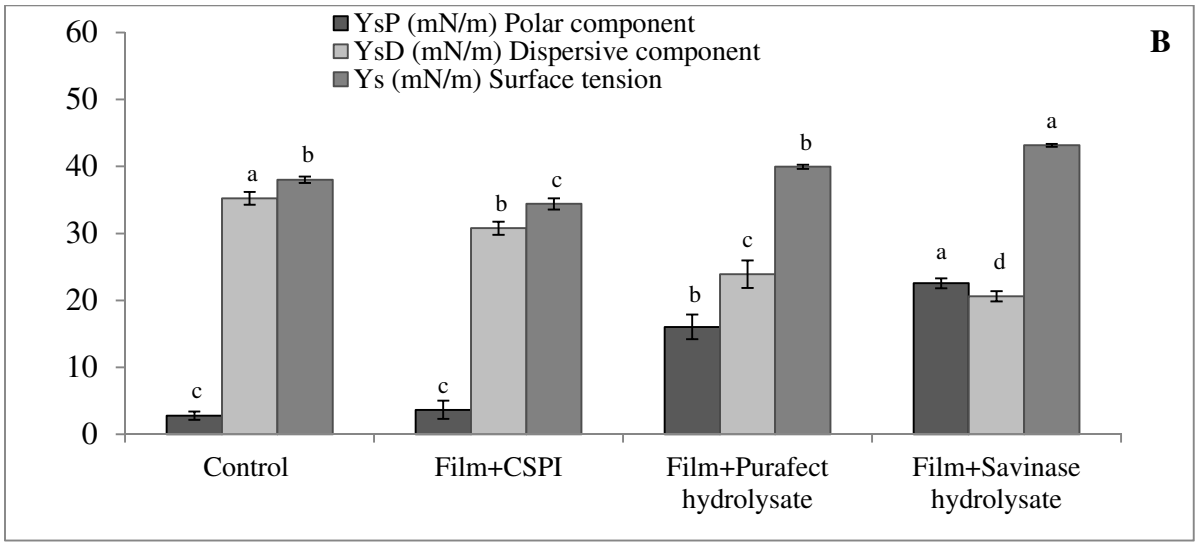
B
YsP (mN/m) Polar component
YsD (mN/m) Dispersive component
Ys (mN/m) Surface tension
60
50
40
30
20
10
0
Control
Film+CSPI
Film+Purafect hydrolysate
Film+Savinase hydrolysate

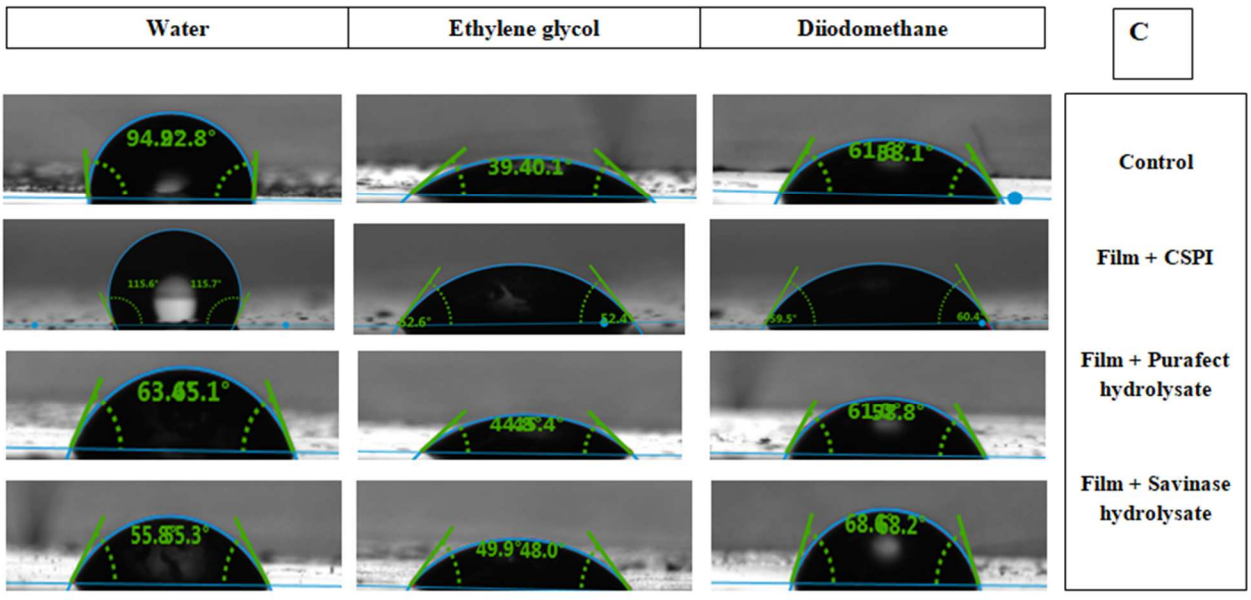
Water
Ethylene glycol
Diiodomethane
C
Control
Film + CSPI
Film + Purafect hydrolysate
Film + Savinase hydrolysate

Fig. 5

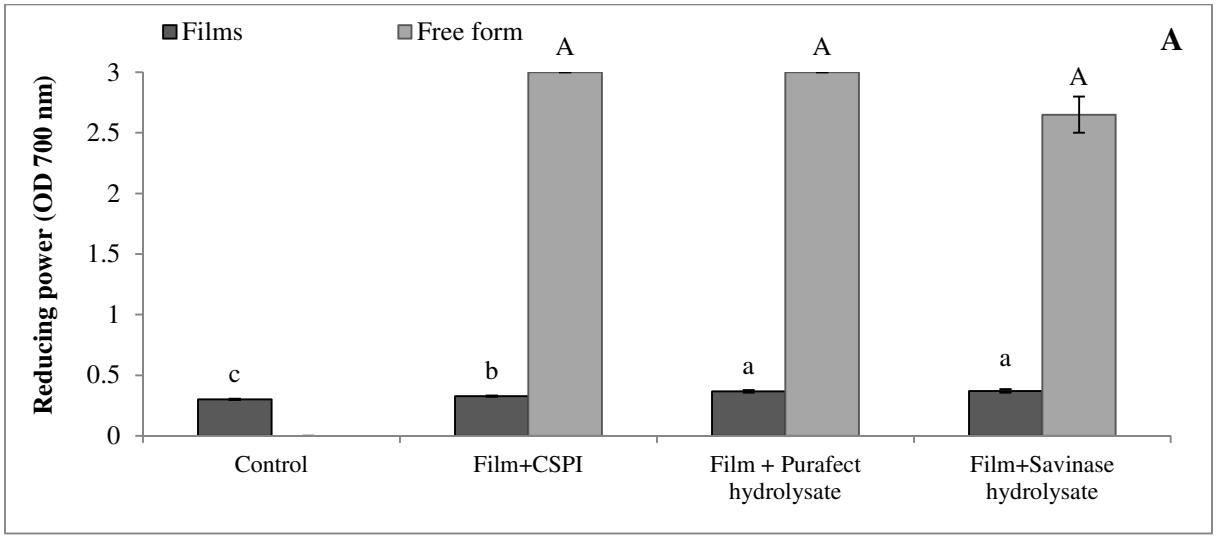
Films
Free form
A
Reducing power (OD 700 nm)
3
2.5
2
1.5
1
0.5
0
c
b
a
a
A
A
A
Control
Film+CSPI
Film + Purafect hydrolysate
Film+Savinase hydrolysate

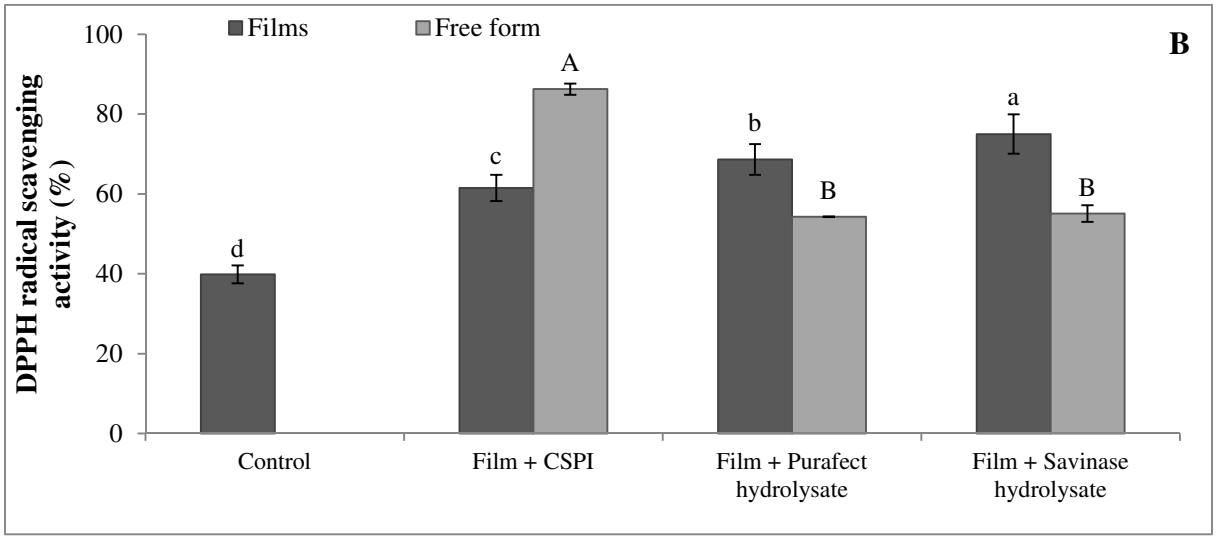
Films
Free form
B
DPPH radical scavenging activity (%)
100
80
60
40
20
0
d
c
b
a
A
B
B
Control
Film + CSPI
Film + Purafect hydrolysate
Film + Savinase hydrolysate

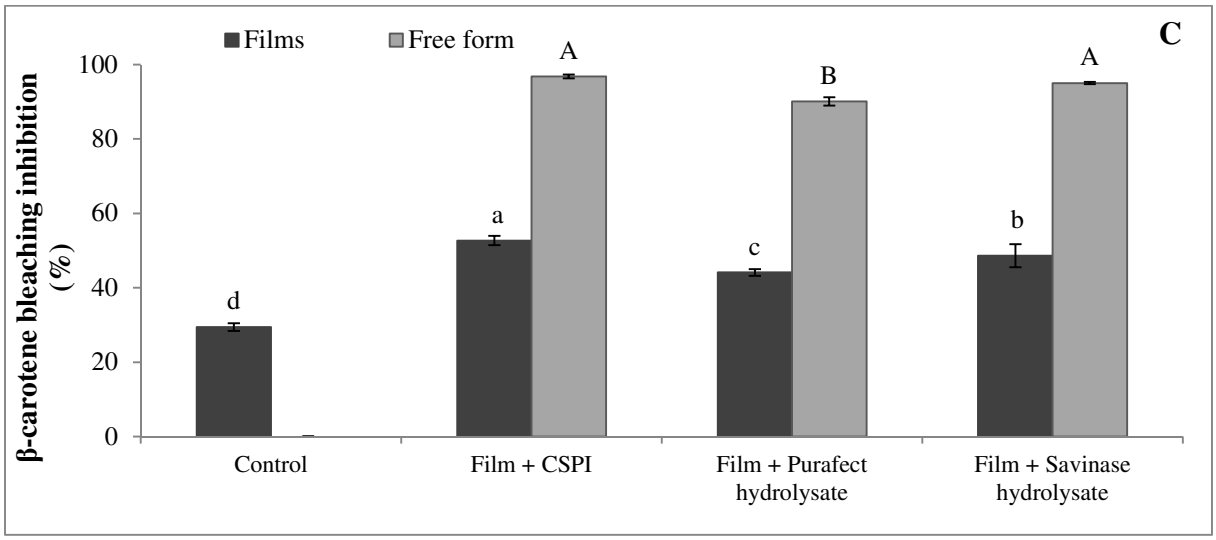
Films
Free form
C
β-carotene bleaching inhibition (%)
100
80
60
40
20
0
d
a
c
b
A
B
A
Control
Film + CSPI
Film + Purafect hydrolysate
Film + Savinase hydrolysate

Table 1: Thickness, color parameters (L*, a*, b*, ΔE*), thermal properties (glass transition temperature Tg, weight loss Δw, thermal degradation temperature T_{max} and residual mass), mechanical properties (Tensile strength TS and elongation at break EAB) of CSG films and those enriched by CSPI and CSPH. All films were previously stored at 25 °C and 50% RH for the determination of the mechanical properties.

Film characterizations		**Control**	**Film + CSPI**	**Film +** Purafect hydrolysate	**Film +** Savinase hydrolysate
Thickness (µm)		84.22±4.01^{a}	79.34±6.07^{a}	75.62±1.56^{a}	77.45±1.34^{a}
Color properties	**L***	89.63±0.12^{a}	85.73±0.42^{bc}	86.27±0.25^{b}	85.43±0.32^{c}
	a*	0.37±0.12^{d}	1.97±1.97^{c}	2.20±0.10^{b}	2.63±0.15^{a}
	b*	3.63±0.23^{c}	7.37±0.45^{b}	7.40±0.10^{b}	8.53±0.21^{a}
	ΔE*	/	5.72±0.57^{b}	5.47±0.11^{b}	6.94±0.07^{a}
Thermal properties *	**Tg (°C)**	58.4^{b}	59.5^{ab}	71.4^{a}	61.8^{ab}
	$\Delta w1$ (%)	14.3	10.9	12.8	12.4
	$\Delta w2$ (%)	64.9	60.5	62.1	62.2
	T_{max} (°C)	296.0	310.7	301.7	297.3
	Residue (%)	18.9	25.7	23.2	23.6
Mechanical properties	**TS (MPa)**	22.67±2.95^{a}	22.09±0.46^{a}	15.85±1.50^{b}	12.29±0.47^{c}
	EAB (%)	32.83±1.97^{a}	26.26±3.51^{b}	10.57±1.28^{c}	10.32±1.39^{c}

Values are given as mean ± standard deviation. Means with different superscripts (a-d) within a same row indicate significant difference ($p<0.05$) in terms of films samples.

* The average relative error on TGA data is lower than 5%

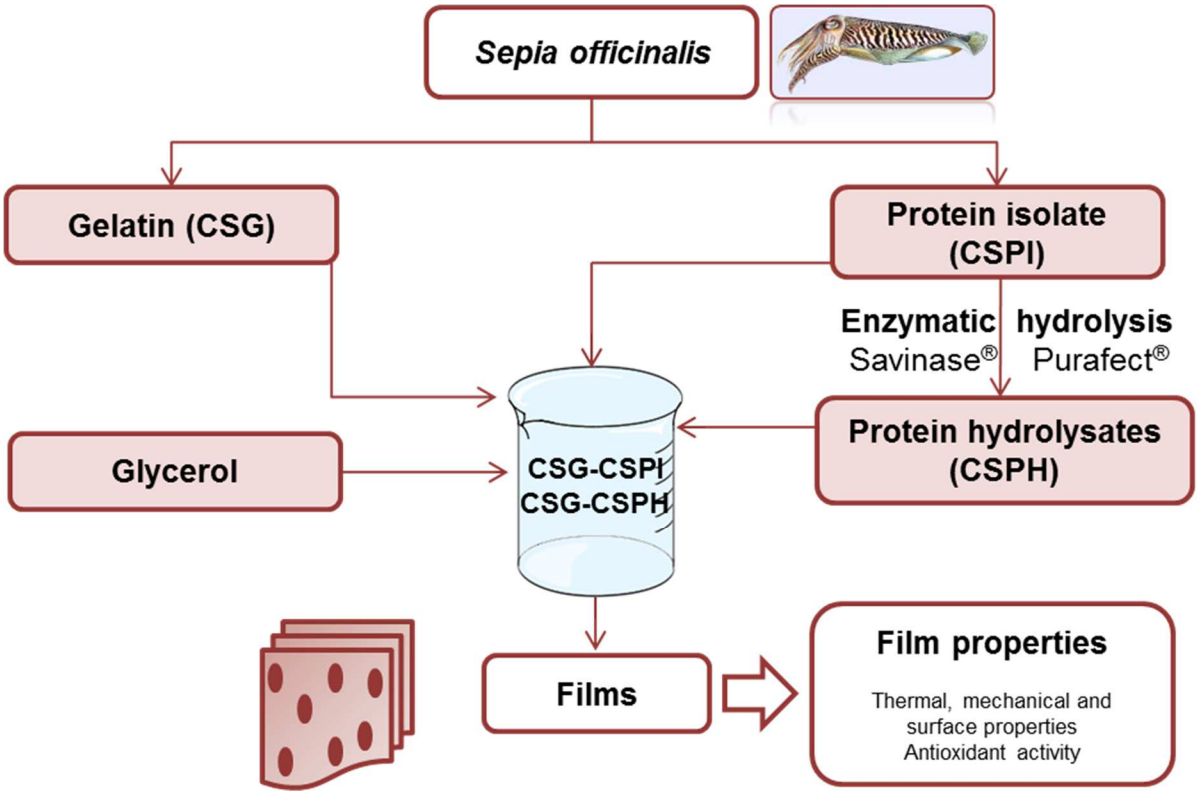
Sepia officinalis
Gelatin (CSG)
Protein isolate (CSPI)
Enzymatic hydrolysis
Savinase®
Purafect®
Protein hydrolysates (CSPH)
Glycerol
CSG-CSPI
CSG-CSPH
Films
Film properties
Thermal, mechanical and surface properties
Antioxidant activity